ISSN 1063-7761, Journal of Experimental and Theoretical Physics, 2017, Vol. 124, No. 5, pp. 779–785. © Pleiades Publishing, Inc., 2017.
Original Russian Text © K.G. Patrin, S.A. Yarikov, G.S. Patrin, V.Yu. Yakovchuk, A.I. Lyamkin, 2017, published in Zhurnal Eksperimental'noi i Teoreticheskoi Fiziki, 2017, Vol. 151, No. 5, pp. 916–923.

ORDER, DISORDER, AND PHASE TRANSITION IN CONDENSED SYSTEM

Magnetic Resonance Studies of Three-Layer FeNi/Bi/FeNi Films

K. G. Patrin[a,b], S. A. Yarikov[a], G. S. Patrin[a]*, V. Yu. Yakovchuk[b], and A. I. Lyamkin[a]

[a] *Siberian Federal University, Krasnoyarsk, 660041 Russia*

[b] *Kirensky Institute of Physics, Siberian Branch, Russian Academy of Sciences, Krasnoyarsk, 660036 Russia*

**e-mail: patrin@iph.krasn.ru*

Received October 18, 2016

Abstract—The interlayer coupling in three-layer FeNi/Bi/FeNi films is studied by electron magnetic resonance. The magnetic anisotropy at the permalloy–bismuth interface is shown to play a significant role in the formation of the magnetic state of the film structure. The interlayer coupling oscillation period is found to be about 8 nm. The interlayer coupling and the interface anisotropy and their temperature dependences are determined.

DOI: 10.1134/S1063776117040069

INTRODUCTION

Multilayer film magnetic structures attract attention of researchers, since materials with unique properties can be created by combining the sequence of magnetic and nonmagnetic layers and by choosing the number of layers in such a structure. The film systems consisting of alternating layers of a ferromagnetic metal and a semiconductor [1] are promising for practical application in spin electronics devices [2, 3]. The interlayer coupling in such systems is responsible for the formation of a magnetic state. If the interlayer coupling can be controlled, new phenomena and effects can take place. If a material with a nonmonotonic type of conduction, namely, a semiconductor, is used as an interlayer material, the properties of the interlayer and the interlayer coupling can be controlled by an external action (impurities, radiation, temperature, magnetic field), which can be used in practice. Although the increases in this field have achieved certain progress, a large number of problems have to be solved. For example, the interface in an Ni/Ge film structure was found to affect the formation of a magnetic state in it [4], a new magnetic state [5, 6] and an additional magnetic anisotropy [7] appear at the Co/Ge interface and degrade the magnetoresistance properties.

Therefore, to create the film structures that could be sensitive to an external action and would have higher coupling between magnetic layers is a challenging problem. One of the methods to solve this problem is thought to be the use of a semimetallic bismuth interlayer instead of a semiconductor material. First, as follows from the phase diagram in [8], most elements in the 3*d* metal–bismuth systems do not form compounds, which ensures a sharp interface between the materials. Second, the electron free path length in bismuth can reach macroscopic scales, and it depends on the layer thickness, the temperature, and the magnetic field. The carrier concentration and mobility also change; as a result, bismuth and its compounds have unusual physical properties in both the bulk [9] and the film [10] state. Most investigations deal with Bi-containing semiconductor alloys as materials for infrared receivers [11] or as multilayer 3*d* metal–bismuth films [12] for microelectromechanical systems (MEMS). A giant magnetoresistance was also detected in three-layer FeNi/Bi/FeNi films [13].

EXPERIMENTAL

Permalloy was chosen as a magnetic material due to its low magnetic crystalline anisotropy for the interlayer coupling not to be shaded. Films with 18 at % Fe and 82 at % Ni were prepared. Two films with different bismuth thicknesses were deposited onto glass substrates in one cycle, and the film from the previous series with a thicker bismuth layer thickness was repeated in two successive process of deposition. The magnetic layer thickness in all films was $t_{NiFe} \approx 10$ nm and the bismuth layer thickness was $t_{Bi} = 4$, 6, 11, and 15 nm. t_{NiFe} was chosen from the considerations that it should be sufficiently small and thick enough for the magnetization of the magnetic layer not to change at layer thickness fluctuations.

The layer thickness was determined by X-ray spectroscopy. Electron-microscopic measurements showed that the layers were continuous over their area and the layer compositions corresponded to the nominal composition. No traces of 3*d* metal–bismuth compounds

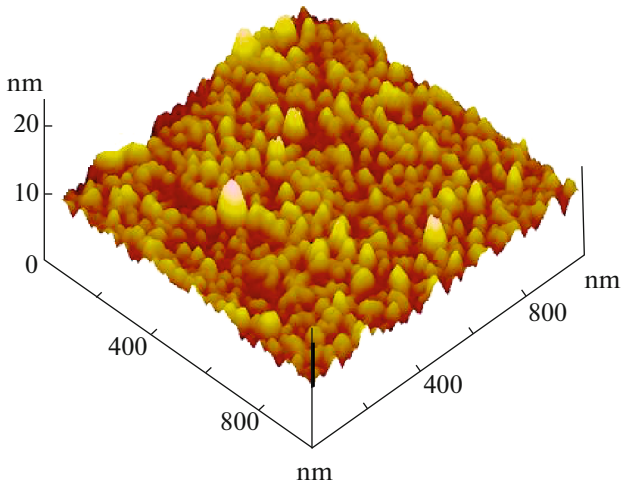

Fig. 1. (Color online) AFM image of an FeNi/Bi/FeNi film with $t_{FeNi} = 10$ nm and $t_{Bi} = 4$ nm.

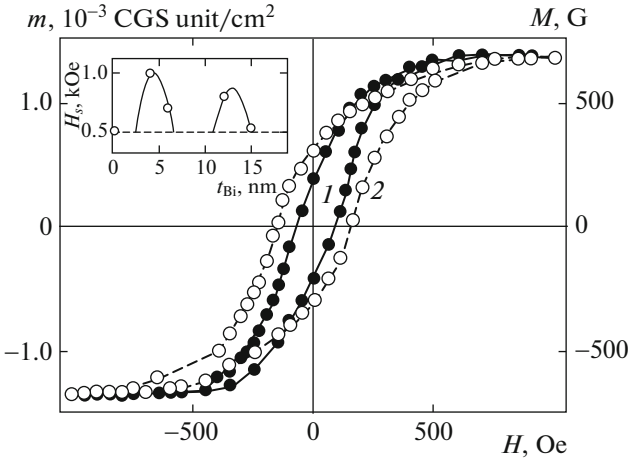

Fig. 2. Hysteresis loops of FeNi/Bi/FeNi films at $T = 4.2$ K: (*1*) without bismuth layer and (*2*) with a bismuth layer of thickness $t_{Bi} = 4$ nm. Left-hand scale, magnetic moment m of unit surface area; right-hand scale, magnetization M. (inset) Saturation field H_s vs. nonmagnetic layer thickness. (points) experimental data and (solid line) fitting by Eq. (2).

were detected. The film surfaces were studied on a Veeco Multi Mode (resolution of 1 nm) atomic force microscope (AFM). The surface roughness did not exceed 2.5 nm (see Fig. 1). This means that no short circuit can occur between neighboring magnetic layers at the given nonmagnetic layer thickness. The magnetization was measured with am MPMS-XL SQUID magnetometer. Magnetic resonance spectra were recorded at a microwave radiation frequency $f_{UHF} = 26.7$ GHz in the temperature range $T = 90$–300 K. A magnetic field lied in the film plane. No resonance field anisotropy was detected in the film plane.

RESULTS AND DISCUSSION

The measurements [13] of the field and temperature dependences of magnetization M of FeNi/Bi/FeNi films showed that the interlayer coupling depended on the bismuth layer thickness. The shape of the $M(H)$ curve was found to change when the bismuth layer thickness increases (Fig. 2). The hysteresis loop of the reference film without a bismuth layer is narrow and the magnetization curve has a standard shape. Figure 3 illustrates the scheme of determining the magnetic saturation field for the films under study. Curve *1* in Fig. 3 corresponds to the part of the magnetization curve that lies in the upper right quadrant of the major hysteresis loop (here, the beginning of saturation for the film with $t_{Bi} = 4$ nm). Curve *2* illustrates the derivative of curve *1*. If a magnetization curve reaches a plateau (true saturation) or exhibits a long "paraprocess," the corresponding derivative is a straight line (not always passing through zero) parallel to the abscissa axis. The saturation field is determined as the point of intersection of the tangential to the derivative (dashed line) and the continuation of this straight line (solid line). This point is designated as H_s in Fig. 3. This method gives good results if it takes a rather long time to reach saturation. If the paraprocess is strong and physically assisted (e.g., strong anisotropy), this situation has to be analyzed separately.

The magnetization saturation field changes in the films with a bismuth layer, and the hysteresis loop width depends nonmonotonically on thickness t_{Bi} (Fig. 4).

If the ferromagnetic layers are assumed to be antiferromagnetically coupled, the data of magnetic measurements can be explained as follows. It is known that magnetic saturation field H_s for antiferromagnetic coupling between ferromagnetic layers is mainly determined by interlayer coupling and has the form [14]

$$H_s = 2H_E \pm H_K, \quad (1)$$

where $H_E = J/t_{FM}M$ is the exchange interaction field for the region of antiferromagnetic coupling; J is the interlayer exchange interaction constant; t_{FM} is the ferromagnetic layer thickness; $H_K = 2K_{in}/M$ is the anisotropy field in the film plane; and signs "+" or "–" in Eq. (1) belong to hard or easy magnetization direction in the film plane, respectively. In our case, we have $K_{in} \approx 0$. In the case of permalloy, the ferromagnetic interlayer coupling should not influence the shape of magnetization, and all specific features are determined by the magnetization of the magnetic material in the magnetic layer. In other words, the magnetization curve should be close to curve *1* in Fig. 2, which is observed in the case at $t_{Bi} = 1.5$ nm (see the inset to Fig. 2).

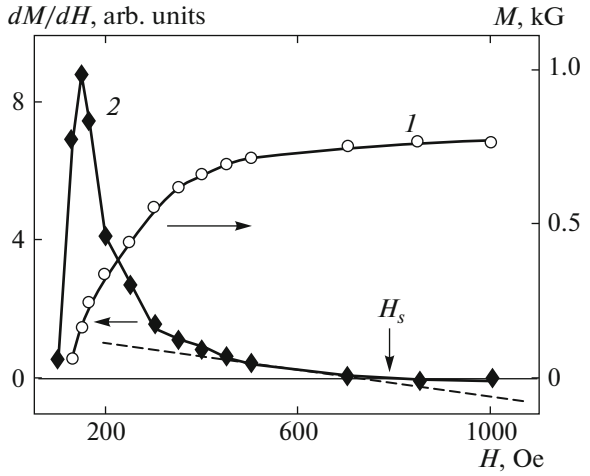

Fig. 3. Scheme for determining the magnetic saturation field: (*1*) ascending branch of the magnetization curve and (*2*) derivative of this segment. $t_{Bi} = 4$ nm.

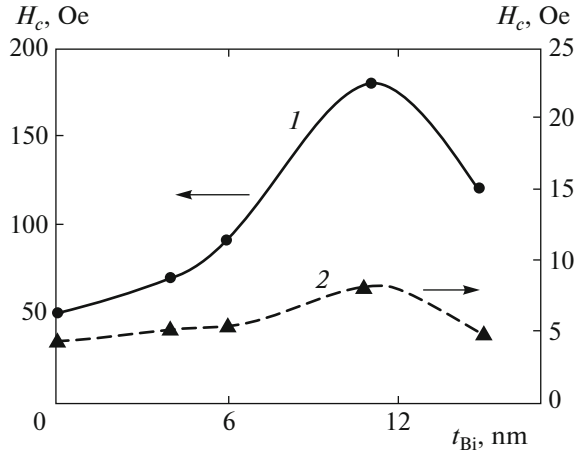

Fig. 4. Coercive force H_c vs. the nonmagnetic layer thickness in FeNi/Bi/FeNi at $T =$ (*1*) 4.2 and (*2*) 300 K.

In the case of ferromagnetic interlayer coupling, a layered structure can affect magnetization processes only because of the imperfection of the interface. It was found [15] that the interface roughness can degrade the situation by smoothing exchange oscillations. This property should be common for all series of films under the same film deposition conditions. In the quantum well approximation (one-dimensional case of charge transfer), the exchange interaction in a three-layer structure as a function of nonmagnetic layer thickness t has an oscillating character and is inversely proportional to this thickness [16]. When processing the experimental data by Eq. (1), we approximated the saturation field by the expression

$$H_s = H_{s0} + B\sin(\alpha t + \varphi)/t^{\beta} \qquad (2)$$

provided $H_s \geq H_{s0}$.

The experimental value of H_s at $T = 4.2$ K for this series of films is well described by the following set of parameters:

$$B = 814, \quad \alpha = 0.747, \quad \varphi = 4.507, \quad \beta = 0.304,$$

$$H_{s0} = 500\,\text{Oe},$$

where H_{s0} is the saturation field of the reference film without a bismuth layer. The fitting results are presented above, in the inset to Fig. 2 (solid lines).

The behavior of the coercive force as a function of the nonmagnetic layer thickness makes it necessary to introduce an interface anisotropy. It is known [17] that the dependence of the anisotropy on the magnetic layer thickness in metallic multilayer films is usually linear (at $t < 5$–10 nm). The sign of anisotropy can be changed in some cases, e.g., in the Co/Pd system [18]. However, the anisotropy constant as a function of the nickel layer thickness in a layered Cu/Ni(110) structure has a nonmonotonic character and has a maximum at $t = 6$ nm [19]. In this case, the change in the anisotropic properties is attributed to an interface contribution. Also note the oscillating behavior of the coercive force in two-layer Bi/Co films as a function of the bismuth layer thickness, and the oscillation period is about 3 nm [20].

Thus, the data of magnetostatic measurements suggest that the interlayer coupling in the FeNi/Bi/FeNi films as a function of the bismuth layer thickness has an oscillating character, which allows us to assume antiferromagnetic exchange between the ferromagnetic layers and the appearance of an additional interface-induced anisotropy. At present, the influence of an interface anisotropy on the magnetization of multilayer structures has been poorly understood.

We used electron magnetic resonance to study the change in the interlayer coupling caused by a change in the temperature or the nonmagnetic layer thickness.

It was found [21] that the microwave absorption curves of the reference film without a bismuth layer and the film with $t_{Bi} \approx 15$ nm have the shape of a single Lorentz line (Fig. 5a). In the bismuth layer thickness range $t_{Bi} = 3$–11 nm, the magnetic resonance spectrum consists of two lines, which indicates a possible antiferromagnetic character of the interlayer coupling between the ferromagnetic layers (see Fig. 5b). We obtained the temperature dependences of the resonance fields and used them to find the temperature dependences of the anisotropy field and the exchange field. Figure 6 shows the temperature dependences of the resonance fields for low- and high-field oscillation modes. The temperature dependences of the low-field are seen to be almost linear, and the high-field lines

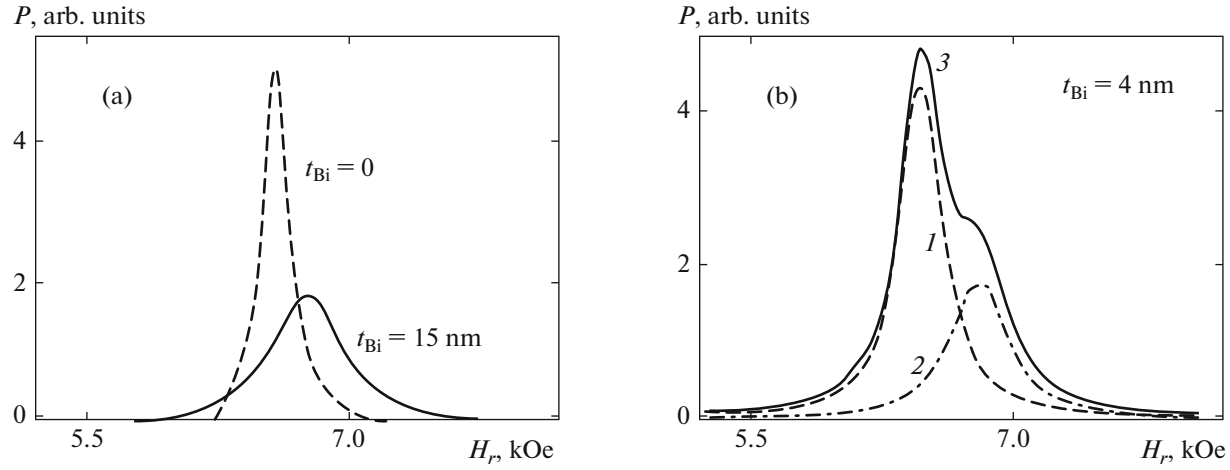

Fig. 5. Electron magnetic resonance spectra at $T = 228$ K for t_{Bi} = (a) 0.15 and (b) 4 nm. (b): (*1*, *2*) resonance lines and (*3*) their resulting line.

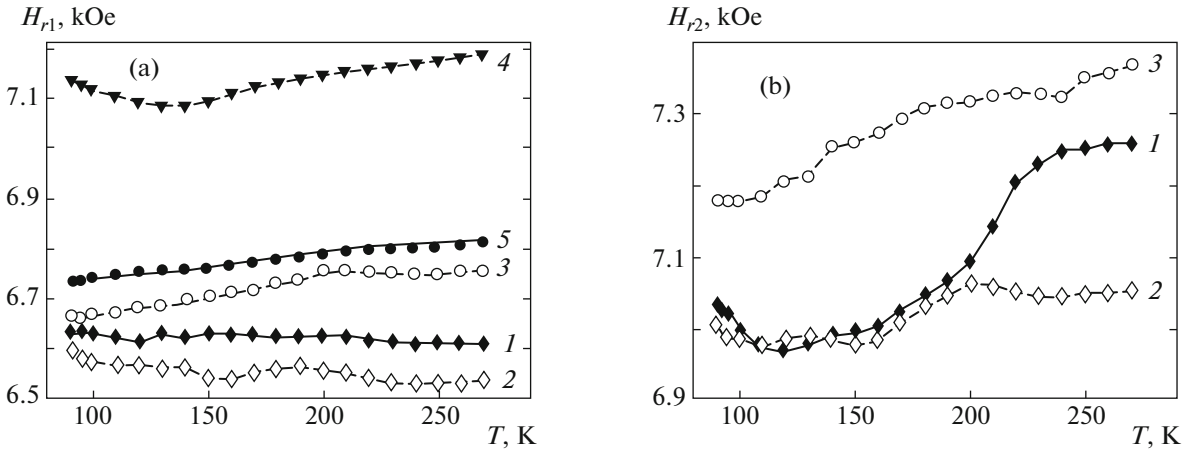

Fig. 6. Temperature dependences of the resonance field in FeNi/Bi/FeNi films: (a) low-field peak (Fig. 2, curve *1*) and (b) high-field peak (Fig. 2, curve *2*). (*1*–*5*) t_{Bi} = 4, 6, 11, 15, and 0 nm, respectively. Curve *5*: (points) experimental data and (solid line) calculation by Eq. (1).

for the films with $t_{Bi} = 4$ and 6 nm have specific features at $T \approx 200$ K.

To determine the parameters that are responsible for the behavior of the magnetic resonance parameters, we processed the experimental results by fitting the magnetic resonance parameters for a three-layer magnetic film. As applied to our case with allowance for the magnetostatic data (for a magnetic field lying in the film plane), the expression for the free energy per unit area has the form [22]

$$E = E_J + E_Z + E_N + E_A, \quad (3)$$

where $E_J = -J\cos(\varphi_1 - \varphi_2)$ is the interlayer coupling energy, $E_Z = -t_{FM}\mathbf{H}(\mathbf{M}_1 + \mathbf{M}_2)$ is the Zeeman interaction energy, $E_N = 2\pi t_{FM}(M_{1z}^2 + M_{2z}^2)$ is the energy related to the shape anisotropy, $E_A = K_1 M_{1z}^2 + K_2 M_{2z}^2$ is the assumed magnetic anisotropy energy of the interface (per unit surface area [23]), $\mathbf{H}$ is the applied magnetic field, $\mathbf{M}_i$ is the magnetization of the ith ferromagnetic layer, φ_i is the magnetization angle in the film plane (measured from the applied magnetic field direction $\varphi_H = 0$), $i = 1$ or 2 is the ferromagnetic layer number, t_{FM} is the magnetic layer thickness, and axis z is perpendicular to the film plane. The values and signs of J and K_i will be determined upon fitting. In the calculation, we assume that $t_{FM}HN \gg J$ and the ferromagnetic layers are in a saturated state, so that $\varphi_i \approx \varphi_H$ (since $H_s \ll H_r$). Both ferromagnetic layers are also assumed to be identical (this assumption is supported by the fact that the saturation magnetizations of the

films from this series coincide with each other). Under these conditions, the resonance frequencies are [22]

$$(\omega_1/\gamma)^2 = H(H + H_A + H_M), \quad (4)$$

$$(\omega_2/\gamma)^2 = H(H + H_A + H_M) + 2(2H + H_A + H_M)H_E + 4H_E^2, \quad (5)$$

where

$$H_M = 4\pi M, \quad K_i = K, \quad H_A = 2K/t_{FM}M, \quad (6)$$

γ is the gyromagnetic ratio, and field H_E was introduced earlier. Since the values of ω, H, and M are known from experiments, we can use Eqs. (4) and (5) to fond H_A and H_E and use Eq. (6) to determine anisotropy constant K and interlayer coupling constant J.

First of all, we analyzed the results belonging to the reference FeNi film (without bismuth layer) of thickness $2t_{FM}$. In the further calculations, we used the dependence obtained for the magnetization of the reference film, since the saturation magnetization is almost the same for all films under study. It was found that the temperature dependence of the resonance field (H_{r1}) for the reference film that was calculated by Eq. (4) passes through experimental points at a high accuracy (Fig. 6a, curve *5*). We obtained $H_A \approx 0$ within the limits of experimental error. This results suggests that the material of the magnetic layer is almost isotropic and that an in-plane magnetic texture is absent.

However, the attempts to analyze the dependences of the resonance fields of the films with a bismuth layer with allowance for only the interlayer exchange without regard for additional contributions did not allow us to obtain reasonable results. It is known [23] that a magnetic anisotropy often appears at the interface in a film structure in addition to the interactions characterizing the layer materials, and this anisotropy can be comparable with the anisotropy of the magnetic material. The interface anisotropy is caused by the fact that elements are mixed at the interface and the nearest environment of magnetic ions changes correspondingly, which brings about a contribution to the anisotropy that differs from the contribution in the bulk state [24]. Obviously, the interface thickness depends on the film deposition conditions and the reactivities of the elements.

If the low-field resonances in the case of films with a bismuth layer are attributed to acoustic modes (see Fig. 6), it follows from the curves in Fig. 6a and Eq. (4) that an easy-plane interface anisotropy is added to the shape anisotropy, which leads to a decrease in the resonance fields. If the high-field signals are assumed to be acoustic modes, the interface anisotropy should be perpendicular to the film plane. We analyzed both possibilities.

The low-field lines in the magnetic resonance spectrum are considered to be acoustic modes.

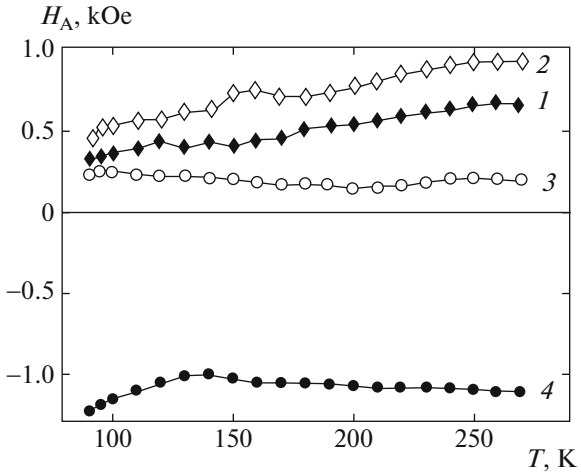

Fig. 7. Temperature dependences of the anisotropy field for FeNi/Bi/FeNi films at t_{Bi} = (*1*) 4, (*2*) 6, (*3*) 11, and (*4*) 15 nm.

Figure 7 shows the temperature dependences of the anisotropy field for the films with a nonmagnetic layer thickness t_{Bi} = 4, 6, and 11 nm. Magnetic anisotropy H_A oscillations are visible. Another fact is of interest: the anisotropic increases with temperature. This behavior was earlier observed in rare-earth metal–3*d* transition metal compounds, e.g., $PrCo_5$ and metallic gadolinium [25]. The effect in these systems is caused by different temperature dependences in the subsystems (4*f* or 3*d* ions) with competing anisotropies or a specific location of energy levels. Such behavior can also exist in film structures [26]. For example, the anisotropy, a change in the sign of interface anisotropy, and the temperature behavior of a Co_m/Cu (*m* is the number of layers) film structure were shown to depend on the interface thickness [24]. Here, the effect is induced by the competition of the contributions of the anisotropic exchange of collective electrons and single-ion anisotropy, and the result depends on number *n*, i.e., the thickness and structure of the interface.

Allowing for the interface anisotropy obtained for the films with t_{Bi} = 4, 6, and 11 nm, we calculated exchange fields H_E that are responsible for interlayer coupling using Eq. (5) (see Fig. 8). First, the sign of interlayer coupling at the calculated values of H_A corresponds to antiferromagnetic coupling. Second, the absolute value of the exchange field increases with temperature (see Fig. 8).

Only one resonance peak is observed for the film with t_{Bi} = 15 nm. The following scenario is possible here. As is seen from the inset to Fig. 2, the saturation field for the film with t_{Bi} = 15 nm is close to H_s of the reference film. This fact means that the interlayer exchange is either zero or ferromagnetic. As is seen in Fig. 4, the coercive force of the film with t_{Bi} = 15 nm is

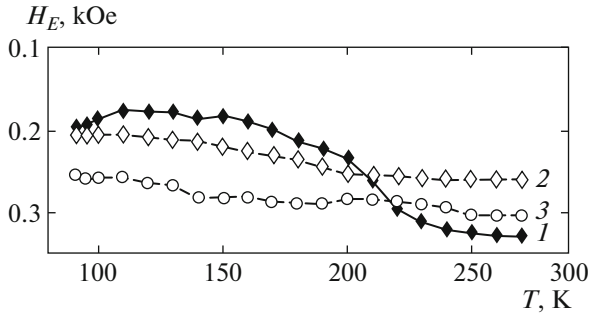

Fig. 8. Temperature dependences of the exchange field for FeNi/Bi/FeNi films at t_{Bi} = (*1*) 4, (*2*) 6, and (*3*) 11 nm.

approximately twice as high as that of the reference film at $T = 4.2$ K (curve *1*), and these forces are almost the same at room temperature (curve *2*). Assuming that the interlayer exchange interaction is zero, we find that the interface anisotropy, which tends to raise the magnetization vector from the film plane, is negative. In this case, we have curve *4* in Fig. 7, and the line belonging to the film with layer thickness $t_{Bi} = 15$ nm in Fig. 5 corresponds to the degenerate resonances of each ferromagnetic layer.

Figure 9 shows the frequency–field dependences of the magnetic resonance in the film with $t_{Bi} = 4$ nm with parameters H_A and H_E calculated by Eqs. (4) and (5) at $T = 150$ K. It is seen that the applied magnetic field almost suppresses both the anisotropy effect and the interlayer exchange effect at the frequency under study and that the $\omega(H)$ functions are linear. The shaded region in Fig. 9 corresponds to the unsaturated magnetic state of the three-layer structure, i.e., to the situation where the condition $H_r < H_s$ is met.

CONCLUSIONS

When performing magnetic resonance investigations, we found that the permalloy–bismuth interface generates an additional anisotropy, which changes its sign depending on the nonmagnetic bismuth layer thickness. At a small bismuth layer thickness, the interface anisotropy is an easy-plane anisotropy, and an easy-axis anisotropy takes place at $t_{Bi} \geq 15$ nm. Since interface anisotropy oscillations were detected at a small bismuth layer thickness and the anisotropy increased with temperature, the interface anisotropy is assumed to be mainly contributed by the anisotropic exchange of collective electrons [24].

The interlayer coupling also has an oscillating character as a function of the bismuth layer thickness. The oscillation period is about 8 nm, which agrees with the data obtained for CoFe/Bi/Co films on the order of magnitude [27, 28]. The interlayer coupling weakly depends on temperature (at $T > 80$ K), and this dependence is most pronounced for films with a small bismuth layer thickness ($t_{Bi} = 4$ nm).

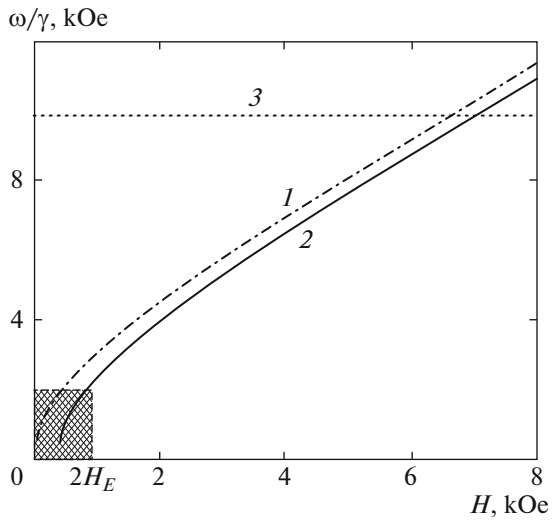

Fig. 9. Frequency–field dependences of the magnetic resonance in an FeNi/Bi/FeNi film with $t_{Bi} = 4$ nm at $T = 150$ K: (*1*) acoustic mode, (*2*) optical mode, and (*3*) the value corresponding to the resonance frequency. The region of an unsaturated magnetic state is shaded.

ACKNOWLEDGMENTS

This work was performed in terms of a state task of the Ministry of Education and Science of the Russian Federation to Siberian Federal University (project no. 3.2534.2014/K) and was supported by the Russian Foundation for Basic Research (project no. 14-02-00238).

REFERENCES

1. G. S. Patrin and V. O. Vas'kovskii, Phys. Met. Metallogr. **101** (Suppl.), S63 (2006).
2. B. T. Jonker, in *Ultrathin Magnetic Structures IV. Applications of Nanomagnetism,* Ed. by B. Heinrich and J. A. C. Bland (Springer, Berlin, 2005), p. 19.
3. M. R. Hofmann and M. Oestreich, in *Magnetic Heterostructures, Advances and Perspectives in Spinstructures and Spintransport,* Ed. by H. Zabel and S. D. Bader (Springer, Berlin, 2008), p. 335.
4. Yu. E. Greben'kova, A. V. Chernichenko, D. A. Velikanov, I. A. Turpanov, E. Kh. Mukhamedzhanov, Ya. V. Zubavichus, A. K. Cherkov, and G. S. Patrin, Phys. Solid State **54**, 1494 (2012).
5. D. A. Muzychenko, K. Schouteden, and C. van Haesendonck, Phys. Rev. B **88**, 195 (2013).
6. G. S. Patrin, V. K. Maltsev, I. N. Krayukhin, and I. A. Turpanov, J. Exp. Theor. Phys. **117**, 1097 (2013).
7. G. S. Patrin, A. V. Kobyakov, I. A. Turpanov, K. G. Patrin, and M. Rautskii, Phys. Solid State **58**, 1034 (2016).
8. V. M. Denisov, N. V. Belousova, G. S. Moiseev, et al., *Bismuth-Containing Materials. Structure and Physicochemical Properties* (UrORAN, Yekaterinburg, 2000) [in Russian].

9. Yu. T. Levitskii, V. I. Palazhchenko, and N. V. Levitskaya, *Semimetals, their Alloys and Compounds* (Dal'nauka, Vladivostok, 2004) [in Russian].
10. Yu. F. Komnik, *Physics of Metallic Films* (Atomizdat, Moscow, 1979) [in Russian].
11. S. J. Sweeney, I. P. Marko, S. R. Jin, et al., in *Bismuth-Containing Compounds,* Ed. by H. Li and Z. M. Wang (Springer, London, 2013), p. 29.
12. T. Hozumi, P. LeClair, G. Mankey, et al., J. Appl. Phys. 115, 17A737 (2014).
13. K. G. Patrin, V. Yu. Yakovchuk, G. S. Patrin, and S. A. Yarikov, Solid State Phenom. **190**, 439 (2012).
14. K. Pettit, S. Gider, S. S. P. Parkin, and M. B. Salamon, Phys. Rev. B **56**, 7819 (1997).
15. Y. Wang, P. M. Levy, and J. L. Fry, Phys. Rev. Lett. **65**, 2732 (1990).
16. M. D. Stiles, in *Ultrathin Magnetic Structures III. Fundamentals of Nanomagnetism*, Ed. by J. A. C. Bland and B. Heinrich (Springer, Berlin, 2005), p. 99.
17. M. T. Johnson, P. J. H. Bloemen, F. J. A. den Broeder, and J. J. DeVrist, Rep. Progr. Phys. **59**, 1409 (1996).
18. S. T. Pursel, M. T. Johnson, N. W. E. McGee, et al., J. Magn. Magn. Mater. **113**, 25 (1992).
19. R. Jungblut, M. T. Johnson, J. van de Stegge, et al., J. Appl. Phys. **75**, 6424 (1994).
20. Jen-Hwa Hsu, Zhi-Long Xue, Ta-Chieh Huang, et al., J. Magn. Magn. Mater. **310**, 2239 (2007).
21. K. G. Patrin, S. A. Yarikov, V. Yu. Yakovchuk, G. S. Patrin, Yu. P. Salomatov, and V. G. Plekhanov, Tech. Phys. Lett. **41**, 1091 (2015).
22. A. Layadi, Phys. Rev. B **65**, 104422 (2002).
23. M. T. Johnson, P. J. Bloemen, F. J. A. den Droeder, and J. J. DeVries, Rep. Progr. Phys. **59**, 1409 (1996).
24. P. Weinberg, *Magnetic Anisotropies in Nanostructured Matter* (Taylor Francis Group, New York, 2009), p. 93.
25. K. P. Belov, A. K. Zvezdin, A. M. Kadomtseva, and R. Z. Levitin, *Orientation Transitions in Rare-Earth Magnetics* (Nauka, Moscow, 1973) [in Russian].
26. R. Skomski, J. Phys.: Condens. Matter **15**, R841 (2003).
27. Jen-Hwa Hsu and D. R. Sahu, Appl. Phys. Lett. **86**, 192501 (2005).
28. Jen-Hwa Hsu, Zhi-Long Xue, and D. Sahu, J. Appl. Phys. **101**, 09D114 (2007).

Translated by K. Shakhlevich